Acta Biomaterialia 8 (2012) 2517–2528

Contents lists available at SciVerse ScienceDirect

Acta Biomaterialia

journal homepage: www.elsevier.com/locate/actabiomat

Development of injectable, resorbable drug-releasing copolymer scaffolds for minimally invasive sustained ophthalmic therapeutics

Scott D. Fitzpatrick [a,1], M.A. Jafar Mazumder [b,c,1], Benjamin Muirhead [a], Heather Sheardown [a,b,*]

[a] School of Biomedical Engineering, McMaster University, 1280 Main Street West, Hamilton ON, Canada L8S 4L7
[b] Department of Chemical Engineering, McMaster University, 1280 Main Street West, Hamilton ON, Canada L8S 4L7
[c] Department of Chemistry, King Fahd University of Petroleum & Minerals, University Blvd, Dhahran 31261, Saudi Arabia

ARTICLE INFO

Article history:
Received 13 December 2011
Received in revised form 16 February 2012
Accepted 7 March 2012
Available online 13 March 2012

Keywords:
Ophthalmic materials
N-isopropylacrylamide
Resorbable
Drug delivery
Retina

ABSTRACT

Copolymers based on N-isopropylacrylamide (NIPAAm), acrylic acid N-hydroxysuccinimide (NAS) and varying concentrations of acrylic acid (AA) and acryloyloxy dimethyl-γ-butyrolactone (DBA) were synthesized to create thermoresponsive, resorbable copolymers for minimally invasive drug and/or cell delivery to the posterior segment of the eye to combat retinal degenerative diseases. Increasing DBA content was found to decrease both copolymer water content and lower critical solution temperature. The incorporation of NAS provided an amine-reactive site, which can be exploited for facile conjugation of bioactive agents. Proton nuclear magnetic resonance analysis revealed the onset of hydrolysis-dependent opening of the DBA lactone ring, which successfully eradicated copolymer phase transition properties and should allow the gelled polymer to re-hydrate, enter systemic circulation and be cleared from the body without the production of degradation byproducts. Hydrolytic ring opening occurs slowly, with over 85% copolymer mass remaining after 130 days of incubation in 37 °C phosphate buffered saline. These slow-degrading copolymers are hypothesized to be ideal delivery vehicles to provide minimally invasive, sustained, localized release of pharmaceuticals within the posterior segment of the eye to combat retinal degenerative diseases.

1. Introduction

Efficient delivery of pharmaceuticals to the back of the eye is one of the most significant unmet needs of visual health care. Numerous pharmaceuticals show promise for the treatment of posterior segment ocular conditions, including vascular endothelial growth factor (VEGF) antagonists capable of minimizing ocular neovascularization, corticosteroids to combat retinal edema and other promising compounds such as antioxidants and anti-hypertensive drugs [1]. However, conventional drug delivery modalities are inefficient for delivering therapeutically relevant doses of pharmaceuticals to affected tissues in the back of the eye. Delivery of drugs to the posterior segment is made difficult by the isolated nature of the eye, which is separated from systemic circulation by blood ocular barriers, including the blood retinal barrier (BRB) and blood aqueous barrier (BAB) [2]. Furthermore, the eye is a segmented structure with numerous barriers to delivery and effective clearance mechanisms efficiently eliminating pharmaceuticals that successfully reach the posterior segment [2]. Topically applied drugs can enter the anterior chamber by crossing the cornea, or through the conjunctiva and sclera [2] or via the systemic circulation, but must cross the BAB. Clearance from the anterior chamber occurs via aqueous turnover, or by re-absorption into systemic circulation [2]. The half-life of a typical drug within the anterior chamber is ~1 h; however, this varies depending on the properties of the pharmaceutical [3]. Drugs can be introduced into the posterior segment, which houses the light-sensitive retina, through systemic circulation by crossing the BRB, through non-corneal permeation into the uvea, or by direct injection into the vitreous [2], with the latter being the most efficient method of delivering drugs to the posterior eye. Drug clearance from the posterior segment occurs through either the anterior or posterior route; the anterior route involves diffusion across the vitreous and elimination via uveal blood flow and aqueous turnover, whereas elimination via the posterior route requires permeation through the BRB [2].

As a result of the numerous barriers, the effective clearance routes and the segmented nature of the eye, delivery of drugs to the posterior segment is particularly challenging. Topically applied eye drops typically result in less than 5% uptake into the anterior chamber and negligible amounts entering the back of the eye [2]. Furthermore, only an estimated 1–2% of a systemically applied dose crosses the restrictive ocular barriers [4]. Therefore, high systemic doses are required to achieve therapeutic concentrations of drug within the posterior segment of the eye [5]. Additionally, many new pharmaceuticals are protein-based and are therefore not suitable for oral delivery as they are rapidly broken down

* Corresponding author. Tel.: +1 905 525 9140x24794; fax: +1 905 521 1350.
E-mail address: sheardow@mcmaster.ca (H. Sheardown).
[1] These authors contributed equally.

1742-7061/$ - see front matter © 2012 Acta Materialia Inc. Published by Elsevier Ltd. All rights reserved.
http://dx.doi.org/10.1016/j.actbio.2012.03.018

and denatured in the digestive system [6]. Direct injection into the vitreous cavity is a highly efficient technique to introduce therapeutically relevant doses of drug into the vitreous body and retinal tissues while minimizing off-target exposure [5]. However, due to the previously mentioned clearance mechanisms, frequent injections (often every 4–6 weeks) are required to maintain therapeutically relevant concentrations [7]. While intravitreal injections are an acceptable means of delivery, in addition to being inconvenient for the physician and patient, frequent injections are associated with increased risk of complications such as endophthalmitis, cataract formation, vitreous hemorrhage, retinal detachment and patient discomfort [5,8]. Therefore, approaches that safely utilize the intravitreal route to provide sustained localized delivery of therapeutic concentrations of drug and do not require frequent perforation of the eye wall represent an exciting potential to treat numerous debilitating ocular conditions.

We hypothesized that poly(N-isopropylacrylamide) (PNIPAAm), a thermally sensitive intelligent polymer, which undergoes a rapid, reversible phase transition from liquid to gel when heated above a lower critical solution temperature (LCST) of ~32 °C, would serve as an ideal delivery scaffold for posterior segment ocular therapy [9]. PNIPAAm's sub-physiologic LCST allows a liquid polymer/drug solution to be injected directly into the vitreal cavity, wherein a thermally induced phase transition drives the formation of a solid drug depot capable of providing sustained, localized therapy. However, as PNIPAAm is a non-degrading polymer, its introduction into the isolated vitreous would result in its persistence within the eye for the lifetime of the patient, unless surgically removed. Therefore, in an attempt to design clinically relevant materials, there has been an emphasis in recent years on developing degradable or resorbable formulations of PNIPAAm that maintain thermal sensitivity but promote the eventual clearance from the body. Neradovic et al. designed NIPAAm-based copolymers containing hydrolyzable lactate ester groups [10,11]. Hydrolysis of hydrophobic side groups results in an increase in copolymer LCST, which, if raised above body temperature, allows the copolymer to undergo a reverse phase transition and revert to a hydrated liquid state, allowing uptake into the systemic circulation and clearance from the body via the kidneys. Ma et al. developed bioabsorbable NIPAAm copolymers possessing strong mechanical properties through copolymerization with methacrylate-polylactide (MAPLA) and hydroxyethyl methacrylate (HEMA) [12]. Yoshida et al. reported the synthesis of NIPAAm-based copolymers crosslinked with degradable poly(amino acids) [13]. Cui et al. demonstrated that through incorporation of dimethyl-γ-butyrolactone acrylate (DBA), a hydrolysis-dependent ring opening of the DBA lactone side group could result in an increase in the LCST above body temperature, allowing the polymer to re-solubilize and be cleared from the body without the formation of degradation byproducts [14,15]. Furthermore, it was found that copolymers of NIPAAm and DBA yielded slow degrading scaffolds with degradation periods of roughly one year required to increase copolymer LCST above body temperature [14]. Based on these results, we propose that copolymers consisting of NIPAAm and DBA would serve as ideal delivery scaffolds for posterior segment therapeutics capable of providing minimally invasive, long-term localized drug release that will increase the time between injections, and upon exhaustion of the drug, hydrolytic degradation will promote clearance from the eye without the need for surgical intervention. However, these polymers lack synthetic flexibility and have limited potential for bioconjugation and cellular adhesion, which may be useful for the subsequent incorporation of cell adhesion peptides for the development of minimally invasive cell carriers capable of delivering cell-based payloads to the subretinal tissues to combat retinal degeneration. Therefore, in this work, we have synthesized a series of synthetically flexible copolymers based on NIPAAm, DBA, acrylic acid (AA) and acrylic acid N-hydroxysuccinimide (NAS). AA was incorporated to balance the hydrophilic and hydrophobic content of the copolymers and control the LCST while the inclusion of NAS was designed to provide a site capable of facile conjugation with biologically relevant molecules such as drugs or cell adhesive peptides. NAS functionality provides a site for copolymer/drug conjugation, which can theoretically be exploited to obtain controlled release through targeted destruction of copolymer/drug linkage, although this was not utilized in this work. Copolymer synthesis as well as physical, chemical and biological characterization are described herein.

2. Materials and methods

DBA (95%), NAS (⩾90%), benzoyl peroxide (BPO, 97%), dexamethasone (98%) and bovine serum albumin (66 kDa) were purchased from Sigma–Aldrich (Oakville, ON, Canada), and used as received. N-isopropylacrylamide (NIPAAm) (97%) was purchased from Sigma–Aldrich and was purified by recrystallization from a toluene/hexane mixture. AA (99%) was purchased from Sigma–Aldrich, and was purified by passing the monomer through a packed column containing Sigma–Aldrich inhibitor remover to extract the polymerization inhibitor, 4-methoxyphenol (MEHQ). 1,4-dioxane, toluene, hexane, tetrahydrofuran (THF), dimethylsulfoxide (DMSO) and anhydrous ethyl ether were purchased from Caledon Laboratories (Caledon, ON) and used as received. Sodium hydroxide and hydrochloric acid solutions were purchased as concentrates from Anachemia Chemical (Rouses Point, NY, USA), and were prepared by diluting to 1.0 or 0.1 M with deionized water. Deionized water with a resistivity of 18.2 MΩ cm was prepared using a Milli-pore Barnstead water purification system (Graham, NC, USA). Phosphate buffered saline solution (PBS, pH 7.4) was purchased from McMaster University Health Science facilities and used as received. Human retinal pigment epithelial (RPE) cells (CRL-2502) were purchased from ATCC (Manasass, VA, USA). Cell culture medium (DMEM-F12) was purchased from McMaster University Health Science facilities. Fetal bovine serum, 1× glutamate, penicillin-streptomycin, Trypan Blue and sodium bicarbonate were purchased from Gibco (Carlsbad, CA, USA). Cellulose dialysis membranes with molecular weight cutoff (MWCO) values from 1 to 12 kg mol^{-1} were purchased from Spectrum Laboratories Inc. (Rancho Dominguez, CA, USA).

2.1. Synthesis of p(NIPAAm-NAS-AA-DBA) copolymers

Poly(NIPAAm-NAS-AA-DBA) (pNNAD) copolymers were synthesized via free radical polymerization. NIPAAm (3.84 g, 33.95 mmol), NAS (0.287 g, 1.69 mmol), AA (0.244 g, 3.39 mmol), DBA (0.626 g, 3.39 mmol) and BPO (0.103 g, 0.42 mmol, 1 mol.% relative to monomer content) were dissolved in 45 ml 1,4-dioxane to form a 10 wt.% monomer solution (90:4:8:8 molar feed ratio of NIPAAm:NAS:AA:DBA). Dry nitrogen was bubbled through the solution for 15 min. The flask was then sealed and subsequently heated to 70 °C for 24 h in a temperature-controlled oil bath with constant stirring to provide uniform mixing. Following the reaction, the polymer solution was cooled to room temperature and isolated by precipitation in anhydrous ethyl ether (1 l). The resulting polymer, denoted pNNAD-8, wherein the number represents the copolymer DBA content, was dried overnight in a vacuum oven at 50 °C. The copolymer was further purified by repeated precipitation from THF into anhydrous ethyl ether. The purified copolymer was then dried to a constant weight in a vacuum oven at 50 °C. pNNAD-8 yield was 90% (4.5 g).

Copolymerization and purification of similar pNNAD copolymers possessing NIPAAm:NAS:AA:DBA molar feed ratios of

80:4:12:4 (pNNAD-4) and 80:4:4:12 (pNNAD-12) were prepared as described. Copolymer yield of pNNAD-4 and pNNAD-12 was 93% (4.65 g) and 87% (4.35 g) respectively. For in vitro and in vivo testing purposes, pNNAD copolymers were further purified by extensive dialysis in deionized water at 4 °C (3.5 kg mol^{-1} MWCO), then freeze-dried, and stored frozen at −20 °C.

2.2. Material characterization

The pNNAD copolymer structures were characterized using a Thermo Fisher Nicolet 6700 Fourier transform infrared (FT-IR) spectrometer. Copolymer compositions were determined by proton nuclear magnetic resonance (^{1}H NMR) using a Bruker AV 600 spectrometer with DMSO-*d*6 as a solvent. Copolymer molecular weights were determined by gel permeation chromatography (GPC) using a Waters system consisting of a 515 HPLC pump, 717 plus autosampler, three ultrahydrogel columns (0–3, 0–50, 2–300 kDa), and a 2414 refractive index detector. Copolymers were first hydrolyzed via accelerated degradation (as described in Section 2.6) to remove phase transition properties, thereby allowing analysis with aqueous phase GPC. Samples were eluted with 20 mM PBS buffer, 100 mM $NaNO_3$ at pH 7.2 using a flow rate of 0.8 ml min^{-1}, and the system was calibrated with commercially available narrow dispersed molecular weight polyethylene glycol (PEG) standards (Waters, Mississauga, ON).

2.3. Lower critical solution temperature characterization

Characterization of copolymer LCST was carried out using differential scanning calorimetry (DSC, TA Instruments 2910) and UV/vis spectrophotometry (Cary 300). For DSC analysis, the samples were dissolved in PBS to 20% and were heated from 0 to 70 °C at a rate of 2 °C min^{-1} in hermetic pans. The thermal transition temperature was considered to be the temperature at which the maximum endothermal peak in the DSC curve was observed. Copolymer cloud points were observed as a change in transmittance using UV spectrophotometry to verify phase transition temperatures obtained via DSC. Copolymers were dissolved in PBS (10% w/v) and kept at 4 °C for 24 h. The copolymer solutions were then placed in 4 ml UV cuvettes and de-gassed briefly via sonication. The samples were heated from 5 to 45 °C with a heating rate of 1 °C min^{-1} and transmittance was assessed every 30 s.

Glass transition temperatures (T_{gs}) of intact and degraded copolymers (~8 mg) were measured by DSC over a temperature range of −10–200 °C with a heating rate of 10 °C min^{-1}.

2.4. Water content

The water content of the pNNAD copolymers was assessed gravimetrically. Samples were dissolved in deionized water (15% w/v) and placed in pre-weighed polystyrene dishes. The covered dishes were then placed in a 37 °C oven to induce hydrogel scaffold formation. After 6 h, the supernatant surrounding the hydrogel pellets was aspirated and the gels were carefully blotted dry with tissue paper to remove any surface water. The samples were placed back in their respective dishes and weighed to obtain the wet mass. The samples were then dried to constant weight in a 65 °C oven. Water content was assessed using the following equation:

$$\text{Water Content} = \frac{(m_w - m_d)}{m_d} * 100\% \quad (1)$$

where m_w is the wet mass of the hydrogel and m_d is the dry mass.

2.5. Degradation by accelerated hydrolysis

Accelerated hydrolysis, both partial and complete, of the pNNAD copolymers was performed following ISO 10993 [16]. Briefly, solutions of each polymer were prepared in deionized water (20% w/v) in a 20 ml glass vial. The pH was adjusted to 10.5 (with either 0.1 or 1 M NaOH) and the solution placed in an oven at 70 °C. The pH of the polymer solution was adjusted to 10.5 daily. Complete degradation of the copolymers was achieved in 21 days, at which point the pH of the solution remained constant. Fully degraded samples were maintained at pH 10.5 for another three days (24 in total) and collected by dialysis (3.5 kg mol^{-1} MWCO) and freeze-dried. During the degradation process, aliquots were collected periodically, dialyzed and freeze-dried to determine the composition of the partially degraded copolymers. Partially degraded pNNAD samples reported in this paper were collected from copolymers subjected to 10 days of accelerated degradation conditions.

2.6. Copolymer degradation in heated PBS

Copolymers were dissolved in PBS (15% w/v) in pre-weighed 2 ml plastic eppendorf tubes. The samples were dissolved at 4 °C for 24 h, then placed in a 37 °C oven and allowed to gel. After 5, 20, 40, 65 and 130 days of incubation at 37 °C, the supernatant was aspirated and samples were carefully rinsed with pre-warmed Milli-Q water to remove any soluble pNNAD and PBS residue. The rinsed samples were then carefully blotted dry with a tissue paper to remove residual surface water and the resulting polymer wet mass m_{wf} was obtained. The samples were then dried to a constant weight in a 65 °C oven, to obtain the final polymer dry mass, m_{df}. Polymer degradation was determined using the following equation:

$$\text{Mass Remaining} = \frac{(m_{df})}{m_{di}} * 100\% \quad (2)$$

where m_{di} denotes the mass of the initial dry sample.

A Phillips 515 scanning electron microscope (SEM) was used to visualize physical changes in polymer morphology as a function of degradation. Dried polymer samples were collected for each time point of the heated PBS degradation assay and a 10 nm platinum coating was applied to the surface of the degraded copolymer samples to allow surface visualization. Images were captured using Mektech URSA 100 Rev. 1.30 imaging software.

2.7. Dexamethasone release

Dexamethasone was dissolved in PBS to form a 0.1 mg ml^{-1} solution. The pNNAD copolymers were then dissolved to concentrations of 20% w/v (100 mg in 0.5 ml) in the PBS/dexamethasone solution. The samples were cooled to 4 °C until the copolymers had fully dissolved. The drug-infused copolymer solutions were then placed in a 37 °C oven for 2 h to drive scaffold formation and drug entrapment at which point the supernatant was collected and the copolymers were rinsed once with a pre-warmed PBS solution. The PBS wash was then removed and replaced with 1 ml of fresh, pre-warmed PBS. This was taken as time zero for drug release. Aliquots (100 μl) were removed at regular intervals and replaced with an equivalent volume of fresh, pre-warmed PBS. Samples were analyzed using a Waters high performance liquid chromatography (HPLC) system with a 2707 autosampler, 2489 UV spectrophotometer, 1525 binary HPLC pump, Atlantis dC18 5 μm, 4.6 × 100 mm column and Breeze 2 software (Build 2154). The mobile phase, a 40% v/v HPLC-grade acetonitrile in water solution, was passed through a 0.45 μm filter and de-gassed via sonication prior to use. A 1.0 ml min^{-1} isocratic flow-rate was employed with 10 μl sample injection volumes and a 254 nm detection wavelength. Sample concentrations were assessed relative to a standard calibration curve of dexamethasone prepared in mobile phase.

Table 1
Polymer feed ratios, final copolymer composition, degraded copolymer molecular weight determined by GPC, intact copolymer molecular weight calculated from degraded samples and phase transition temperatures determined using DSC.

Polymer (feed ratio) NIPAAM-NAS-AA-DBA	Composition[a]	MW (M_n) (kg mol^{-1})[b] (degraded)	MW (M_n) (kg mol^{-1})[c] (intact)	LCST[d] (intact)	LCST[d] (degraded)	T_g (°C) (intact)	T_g (°C) (degraded)
pNNAD-4 (80:4:12:4)	76.0:4.4:15.1:4.5	26563	28166	21.3	NA	94.3	98.6
pNNAD-8 (80:4:8:8)	74.8:4.1:12.9:8.2	28494	32146	17.0	NA	90.8	97.8
pNNAD-12 (80:4:4:12)	75.2:3.8:8.6:12.4	30776	36034	13.1	NA	87.6	100.9

[a] Copolymer composition in mol.% determined by ^{1}H NMR.
[b] M_n obtained using gel permeation chromatography (GPC).
[c] Calculated from GPC.
[d] LCST obtained from DSC.

2.8. Cell culture

Human RPE cells (CRL-2502) were cultured in a temperature-controlled CO_2 incubator (37 °C, 5% CO_2, 95% air, 100% humidity). DMEM-F12 cell culture medium was supplemented with fetal bovine serum (FBS) (6.25% final concentration), 1× glutamate (1% final concentration), penicillin-streptomycin (1% final concentration), and sodium bicarbonate (0.8% final concentration). Prior to testing, samples were extensively dialyzed in deionized water (3.5 kg mol^{-1} MWCO), freeze-dried and then pre-treated with a solution of PBS and penicillin-streptomycin (3:1 v/v). RPE cells were seeded with fresh, supplemented DMEM-F12 culture medium in a 48-well tissue culture polystyrene (TCPS) dish at a density of 50,000 cells per well. After a 2 h incubation period, which allowed cells to adhere to the bottom of the TCPS dish, the cell supernatant was removed and replaced with 1 ml of fresh medium containing 10 mg of dissolved copolymer. Test conditions included partially degraded, fully hydrolyzed and intact pNNAD-4, pNNAD-8 and pNNAD-12 copolymers. Fresh culture medium containing no polymer was used as a control. Samples were then returned to the incubator and viability was assessed after 96 h using a 0.4% Trypan Blue exclusion assay.

2.9. Subcutaneous injections in SKH1-E and C3H mice

Following extensive dialysis and freeze-drying, samples were sterilized with ethylene oxide (EO) gas at the McMaster University histopathology laboratory for subsequent in vivo testing. Samples were exposed to a 100% EO atmosphere at 57 °C for 2 h followed by exposure to sterile air for 15 h to evaporate residual EO. Copolymers pNNAD-4, pNNAD-8 and pNNAD-12 were dissolved in Fischer Brand medical grade saline to concentrations of 15% w/v in 10 ml aliquots. Polymer samples, syringes and the injection site were pre-cooled with ice to prevent premature polymer gelation during injection. Hairless SKH1-E (strain code 447) or C3H (Charles River, strain code 025) mice were anesthetized with isoflurane gas and 100 μl polymer suspensions were injected subcutaneously above the left flank of the animal. C3H mice were shaved prior to treatment and the injection site was marked with an indelible pen. C3H mice were sacrificed at day 1, 3, 7 ($n = 3$) and SKH1-E mice were sacrificed at day 40 ($n = 2$). The tissue at the injection site was excised, fixed in a 4% formalin solution for 24–72 h and then embedded within paraffin wax. The fixed tissues were then sliced into 4 μm sections using a Leica RM2255 microtome and stained with haemotoxylin and eosin (H&E) or Masson's trichrome following standard histological protocols. Images of the stained and processed tissue from the injection site were captured using an Olympus BX51 optical microscope with a QImaging Retiga 2000R camera and Image-Pro Plus (version 7.0) imaging software. Full liver and spleen samples were excised at day 40 and weighed. All animal testing was performed in accordance with the McMaster University Animal Research Ethics Board.

2.10. Statistical analysis

A one-factor analysis of variance (ANOVA) was used to analyze copolymer water content and RPE viability using an $\alpha = 0.05$. Statistical analysis was performed using PASW Statistics 18 (SPSS Inc., IL). All error bars represent standard deviation.

3. Results and discussion

3.1. Copolymer characterization

Copolymers with varying compositions of NIPAAm, NAS, AA and DBA were synthesized via free radical polymerization. The final composition of the various pNNAD copolymers was determined using ^{1}H NMR and the values, which were found to be similar to the co-monomer feed ratios, are reported in Table 1.

3.2. Physiological and accelerated pNNAD degradation mechanisms

FT-IR was used to confirm the final structure of the various pNNAD copolymers as well as to examine the changes in copolymer structure as a function of accelerated degradation, Fig. 1. The pNNAD-4 spectrum in Fig. 1a shows characteristic NIPAAm peaks of C=O and N–H stretching of the amide groups around 1658 and 1540 cm^{-1} respectively. Additionally, stretching vibration of the N–H amine group appears at 3309 cm^{-1}, and the isopropyl group is present at 1460, 1380, and 1360 cm^{-1} (Fig. 1a↵). Characteristic NAS succinimide peaks were observed at 1812, 1781 and 1735 cm^{-1} (Fig. 1a∗). The carbonyl group from AA was observed at 1710 cm^{-1} (Fig. 1a↓). The two characteristic DBA peaks, specifically the carbonyl peak in the ring structure and the carbonyl peak connected to the polymer backbone, overlap with the succinimide peaks at 1781 and 1735 cm^{-1} respectively.

During the accelerated degradation process, the pH was adjusted to 10.5 daily with 1 M or 0.1 M NaOH. Decreases in the pH of roughly 1 unit were observed in the first few days of the process, and were followed by smaller decreases over the next two weeks until equilibrium was achieved after 21 days, indicating that complete copolymer degradation had been attained. These degraded samples were maintained at pH 10.5 for 3 more days prior to purification and analysis. Following 10 days of exposure to harsh degradation conditions, partial degradation of the pNNAD copolymers was observed to occur through opening of the DBA lactone ring structure, which rendered a decrease in the DBA ring carbonyl peak and an increase in the carboxylic acid C=O peak around 1652 cm^{-1} (Fig. 1b, pNNAD-4 shown). Complete degradation of the pNNAD copolymers resulted in the disappearance of the DBA carbonyl peak and the production of a broad carboxylic acid C=O peak around 1652 cm^{-1} (Fig. 1c), confirming the proposed sequential degradation mechanism.

^{1}H NMR was used to verify the sequential degradation mechanism of the pNNAD copolymers, Fig. 2. In the pNNAD-4 spectra,

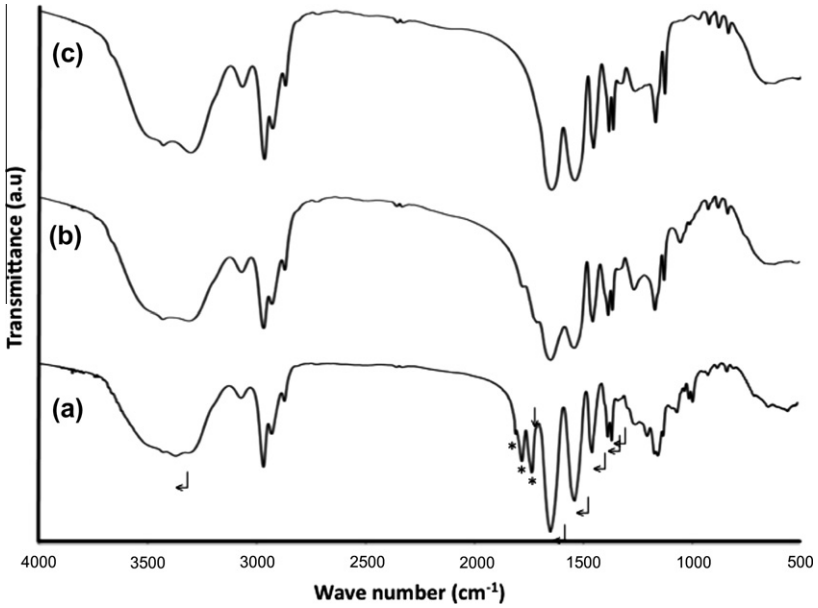

Fig. 1. FT-IR spectra of pNNAD-4 (a), partially degraded pNNAD-4 (b) and completely hydrolyzed pNNAD-4 (c). Both pNNAD-8 and pNNAD-12 displayed a similar sequential degradation mechanism (not shown).

Fig. 2a, two characteristic peaks (CH and CH_2) within the DBA ring can be seen between 5.2–5.7 ppm and 3.8–4.1 ppm respectively. Partial degradation following 10 days of accelerated degradation in harsh basic conditions results in a decrease in the magnitude of these characteristic DBA ring peaks and the CH peak shifts to 4.3–4.7 ppm, Fig. 2b. Furthermore, the new CH_2 peak from the former DBA ring appears at 3.0–3.5 ppm, confirming successful ring opening while the ester linkage remains intact with the polymer backbone. Complete degradation is confirmed in Fig. 2c with the disappearance of these two DBA ring proton peaks (CH and CH_2), while the resulting spectrum is consistent with a poly(NIPAAm-*co*-AA) signature. As expected, both pNNAD-8 and pNNAD-12 show similar degradation trends (data not shown). The proposed copolymer degradation mechanisms of pNNAD under both physiological and harsh basic conditions are illustrated in Scheme 1.

It was proposed that under physiologic conditions, hydrolytic ring opening of the DBA lactone ring structure would significantly alter copolymer phase transition properties as the hydrophobic lactone ring opens to expose hydrophilic carboxylic acid and hydroxyl groups. The resulting increase in copolymer LCST would initiate a reverse phase transition process, inducing the solid cell or drug scaffold to re-hydrate to a liquid state, allowing the copolymer to be cleared from the eye through the available ocular elimination routes. To prolong the duration of drug release within the hard-to-access vitreous, it is desirable to design copolymers with slow degradation kinetics wherein degradation should occur following exhaustion of the majority of drug reservoir to prevent excessive degradation-induced drug dumping. Slow degradation should decrease the secondary burst associated with scaffold degradation, therefore limiting the amount of free drug present within the vitreous and minimizing associated complications such as cataract formation and increases in intraocular pressure (IOP), which can lead to secondary open-angle glaucoma [17,18]. Furthermore, it is desirable to design a copolymer system that does not break down into small-molecular-weight byproducts as these degradation products can be cytotoxic and can induce an inflammatory response [15]. Under physiologic conditions, pNNAD should not produce degradation byproducts as resorption should be achieved through a simple hydrolysis-dependent alteration in copolymer critical gelling temperature. However, under harsh basic conditions, such as that of the accelerated degradation process, the copolymer degradation scheme is more rigorous. Harsh degradation conditions result in the hydrolysis of the DBA ester group attached to the copolymer backbone leading to the conversion of the DBA co-monomer to AA. Both physiologic and harsh degradation conditions liberate the hydroxysuccinimide group from NAS, similarly producing AA. However, bioconjugation of the pNNAD copolymers with cell adhesive peptides would produce stable amide bonds that are not susceptible to degradation. In the absence of bioconjugation, capping NAS functional groups would eliminate the hydrolytic release of hydroxysuccinimide in vivo. The impact of NAS capping on polymer behavior such as degradation kinetics, LCST, drug release kinetics and final copolymer MW will ultimately need to match the design constraints of the system to preserve the desired copolymer properties.

3.3. Water content

The water content of the pNNAD copolymers was assessed gravimetrically and, consistent with thermal transition properties, was found to be strongly dependent on AA and DBA content, Fig. 3. As copolymer DBA/AA ratio increased, the hydrophobic nature of the copolymer increased, thereby decreasing the water content and lowering the LCST.

Glass transition temperatures (Table 1) of intact and degraded pNNAD copolymers were assessed by DSC and found to be dependent on both AA and DBA content. Intact copolymers with a higher AA/DBA ratio were found to have higher T_g due to increased hydrophilicity and increased water content. However, after degradation, all copolymers were reduced to similar NIPAAm and AA content as DBA and NAS groups were hydrolyzed to form AA. As a result, T_g for all copolymers following degradation was approximately the same, providing further evidence for copolymer composition.

3.4. pNNAD copolymer phase transition properties

The copolymer phase transition properties were characterized by both DSC and UV spectrophotometry. LCST values obtained via DSC are reported in Table 1 and the transmittance curves as a function of increasing temperature are shown in Fig. 4. pNNAD

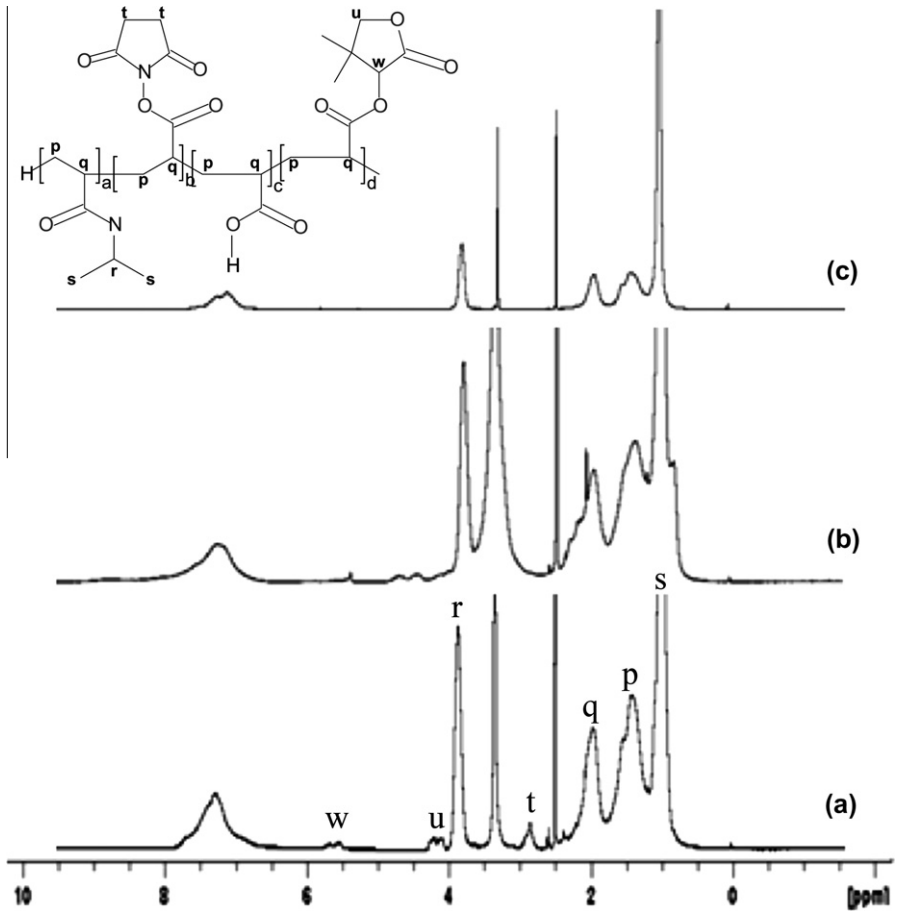

Fig. 2. Sequential degradation spectra of intact pNNAD-4 (a), partially degraded pNNAD-4 (b) and completely hydrolyzed pNNAD-4 (c) copolymers confirmed by ^{1}H NMR. Both pNNAD-8 and pNNAD-12 displayed a similar sequential degradation mechanism (not shown).

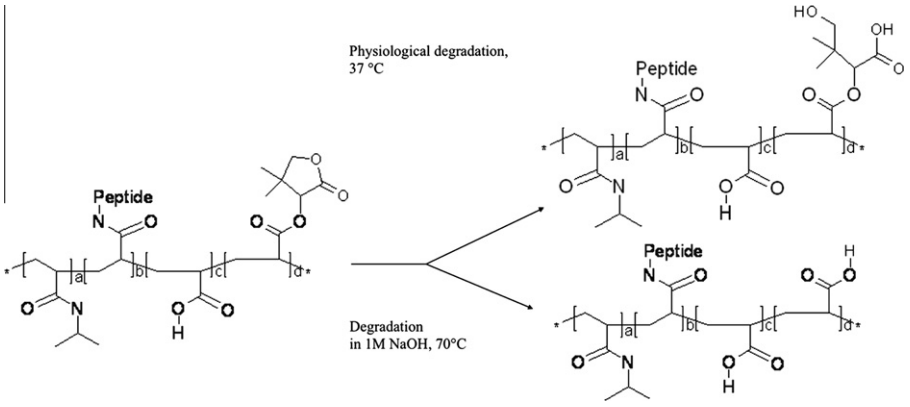

Scheme 1. The sequential degradation mechanism of pNNAD copolymers in physiological conditions (top) and under harsh basic conditions (bottom) employed in the accelerated degradation experiment. In this schematic, the pNNAD copolymer has been functionalized with a peptide through NAS reactivity. In the absence of conjugation, NAS hydrolyzes to produce AA.

LCST values were strongly influenced by DBA and AA content; higher ratios of DBA to AA produced more hydrophobic copolymers, resulting in lower phase transition temperatures. All copolymers were found to have sub-physiological phase transition temperatures, which is a requirement for in situ forming hydrogel scaffolds that utilize body temperature as the stimuli to induce phase transition. The sudden decrease in transmittance as the copolymers are heated above their LCST provides evidence that the copolymers undergo a rapid sol-gel transition, an observation that was verified during in vivo testing in which robust polymer gels were formed almost immediately following subcutaneous injection. Rapid gelling kinetics are important for in situ forming hydrogels in order to efficiently entrap the infused therapeutic. Unlike pre-formed drug releasing scaffolds, which are loaded with drug ex vivo, the pNNAD copolymers are simply mixed with a drug solution and must gel quickly following injection to form a solid drug depot in situ while preventing mass efflux of free drug into the surrounding environment. In situ forming hydrogels that gel

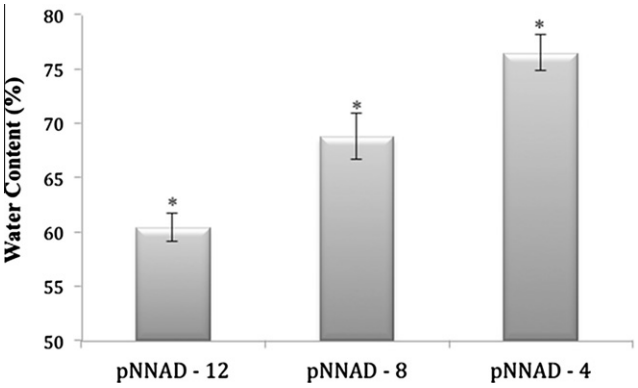

Fig. 3. Water content of the various pNNAD copolymers was measured gravimetrically and found to be highly dependent on AA and DBA content. The difference among mean water content was statistically significant for all samples ($p \leqslant 0.01$).

too slowly do not efficiently entrap the infused drug and are associated with a large initial burst, whereas if gelation occurs too rapidly, it may clog the injection syringe. From our studies, we observed rapid gelation upon injection of 15–20% pNNAD copolymers into pre-heated aqueous solutions and did not suffer syringe clogging when using needles of gauge 18–27 with pre-cooled samples.

The sudden decrease in transmittance, as the copolymers transition from a transparent liquid to an opaque white gel, raises one of the main concerns for the pNNAD copolymers: they are not clear. However, this is not anticipated to be an issue as the pNNAD drug depot will reside on the floor of the vitreous, well outside the visual axis, much like similar non-transparent free-floating intravitreal drug delivery scaffolds, Osurdex (Allergan) and Iluvien (Alimera Sciences).

Following partial and complete degradation via accelerated hydrolysis, there was no observable LCST between 0 and 100 °C as assessed by DSC (Fig. 5b and c respectively). This significant finding demonstrates that the first stages of the sequential pNNAD degradation, which were confirmed by FT-IR and ^{1}H NMR to occur through hydrolytic opening of the DBA ring, are sufficient to eliminate the thermoresponsive nature of the copolymer between 0 and 100 °C. Therefore, as the DBA ring opens, the gelled copolymer will revert to a liquid state, allowing its clearance from the eye, uptake into systemic circulation and ultimate removal from the body via the kidneys, without the liberation of degradation byproducts.

3.5. Copolymer molecular weight

To determine copolymer molecular weight, organic phase GPC was initially selected because temperature-induced phase transition properties in aqueous conditions prevented the use of aqueous phase GPC. However, organic phase GPC with both THF and DMF solvents yielded highly irregular and inconsistent molecular weight measurements with values exceeding 10^6 Da. Therefore, the copolymers were subjected to accelerated hydrolysis to remove phase transition properties, thereby allowing MW assessment via aqueous phase GPC. Copolymer molecular weights are presented in Table 1. As MW measurements were obtained using hydrolyzed pNNAD copolymers, the resulting MW values are slightly lower than fully intact copolymers. However, initial copolymer MW values were quantified using these data by calculating the MW of the hydrolyzed copolymer side groups that were cleaved from the copolymer backbone, Table 1. From these calculations, it can be seen that all pNNAD copolymers possess an initial MW below the molecular weight cutoff of the renal system, which has been reported to have an upper limit of ~50 kDa [19]. Therefore, intact pNNAD copolymers possessing sufficient quantities of hydrolytically opened lactone ring structures to increase copolymer LCST above body temperature should be readily filtered from the body via the kidneys without the formation of degradation byproducts.

3.6. Copolymer degradation studies

Copolymer degradation kinetics were studied by dissolving pNNAD copolymers in PBS (15% w/v). The samples were maintained in a 37 °C incubator for 5, 20, 40, 65 and 130 days, at which point, the supernatant was aspirated to remove PBS as well as any pNNAD copolymer that had transitioned back into a soluble state. The samples were then carefully rinsed with pre-heated deionized water to remove residual PBS and hydrolyzed pNNAD. The copolymers were dried to constant weight and the mass remaining was calculated using Eq. (2), Fig. 6.

From Fig. 6, it is apparent that hydrolytic ring opening of the DBA side chain occurs slowly in vitro as all scaffolds maintained

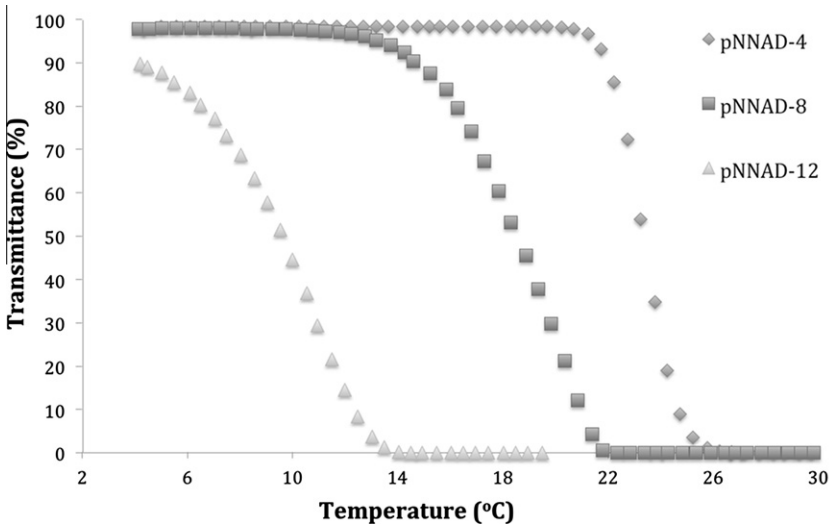

Fig. 4. Transmittance measurements of the various pNNAD copolymers as a function of increasing temperature demonstrate rapid gel formation at LCST values similar to that observed via DSC.

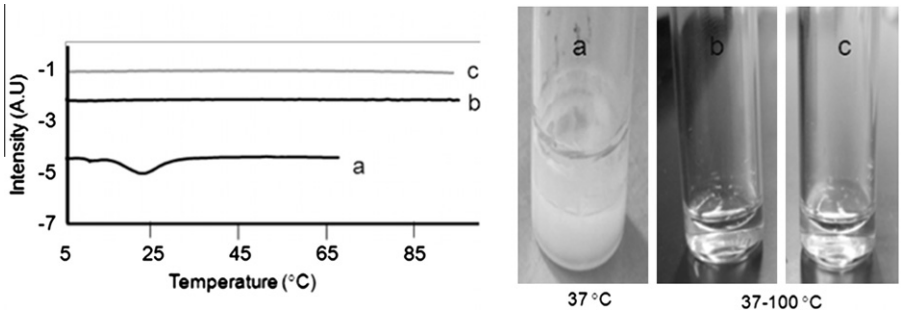

Fig. 5. DSC analysis (left image) revealed an LCST commencing at ~21 °C for intact pNNAD-4 (a) and the complete removal of phase transition properties following partial degradation (b) and complete hydrolysis (c) in harsh basic conditions.

over 85% of their initial mass following 130 days in heated PBS. As discussed, this slow degradation is highly favorable for ocular drug delivery as it may be conducive to providing long-term sustained release of low-levels of drug, minimizing the frequency of intravitreal injections. It is expected that degradation will occur more rapidly in an in vivo environment in which harsher conditions can expedite the hydrolytic process. Therefore, future studies will examine copolymer degradation kinetics within the vitreous.

SEM images of the dried pNNAD copolymers were collected at each time point to assess changes in morphology as a function of degradation, Fig. 7. Though oven drying can introduce artifacts into polymer morphology, these effects would be consistent for all samples and would likely manifest as surface fractures as the polymers dry. Such fractures as can be observed in the pNNAD-4 day 20 sample should therefore not be interpreted as evidence of degradation.

The SEM micrographs reveal subtle changes in copolymer morphology as a function of time in the heated PBS conditions. Morphological changes in the copolymer surface are most apparent in pNNAD-4, which has the lowest DBA content and highest water content. There is evidence of increased pitting and surface erosion in pNNAD-4, and to some extent pNNAD-8, at day 130. As expected, surface degradation in the pNNAD-12 copolymer, which has the highest DBA content and lowest water content, appears to be less evident than the other two materials. The pNNAD-8 and pNNAD-12 day 40 images were taken of fractures that occurred as a result of sample handling that exposed internal copolymer morphology. The internal copolymer structure does not reveal the same pitting morphology observed on the surface, possibly indicating that erosion occurs primarily on the surface, where there is the greatest amount of water present to expedite the process of lactone ring hydrolysis.

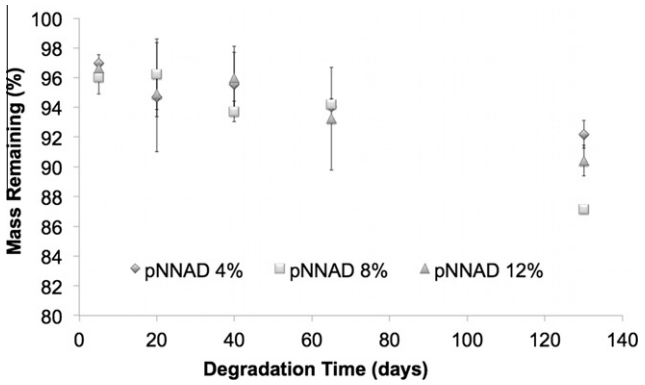

Fig. 6. Slow pNNAD copolymer degradation kinetics were revealed by assessing mass loss as a function of time in 37 °C PBS. Slow degradation may allow for sustained release of low levels of pharmaceuticals, which ultimately is desired to decrease the frequency of intravitreal injection.

However, none of the copolymers undergoes dramatic morphological changes over the course of 130 days in heated PBS, which is consistent with the relatively minor mass loss observed throughout the course of the experiment. As the copolymers continue to hydrolyze, their surfaces will erode and become more porous, increasing the surface area through which drugs can diffuse, which in turn increases the release rate. For long-term sustained release applications, slow degrading materials that do not undergo rapid changes in morphology are desirable to maintain relatively controlled release rates for extended periods of time. Therefore, the minimal surface erosion and slow degradation kinetics exhibited by the pNNAD copolymers, specifically pNNAD-12, appear to support the hypothesis that these materials would provide desirable vehicles for long-term release of pharmaceuticals in ophthalmic therapeutics.

3.7. Dexamethasone release

Corticosteroids are thought to combat macular edema through anti-inflammatory and anti-angiogenic properties, the latter of which occurs through suppression of vascular endothelial growth factor (VEGF) expression, which has been shown to play a key role in ocular neovascularization [20]. Corticosteroids are also capable of stabilization of the BRB [20]. As mentioned, free steroid suspensions within the eye can cause a number of complications, such as cataract and glaucoma formation. However, entrapment within a scaffold that slowly releases low levels of drug for sustained periods of time can significantly decrease the amount of free drug present within the vitreous and greatly decrease the associated risk [21]. To examine release kinetics from the pNNAD scaffolds, dexamethasone was selected as the model drug since it is one of the most attractive corticosteroids for the treatment of posterior complications, specifically macular edema [22]. Triamcinolone acetonide (TA) is the most commonly used intravitreal corticosteroid; however, its use is associated with a relatively high rate of cataract formation and glaucoma [22]. Dexamethasone is five times more potent than TA and studies suggest it may be associated with a decreased risk of cataract, glaucoma and retinal toxicity [22]. Relative to TA, dexamethasone displayed lower toxicity towards lens epithelial cells [23], trabecular meshwork cells [22,24] and retinal neurosensory and RPE cells [25,26] in vitro. However, dexamethasone (392.5 Da) suffers from a relatively short half-life within the eye (3.5 h), whereas TA (18 days) has been shown to persist for 3 months [27–29]. Therefore, releasing dexamethasone from a slow-releasing pNNAD scaffold (similar to Osurdex [30]) should help create persistent levels of the potent corticosteroid within the eye, extending its duration of action, minimizing the number of repeat injections required to maintain therapeutic concentrations and lower the incidence of steroid-related complications.

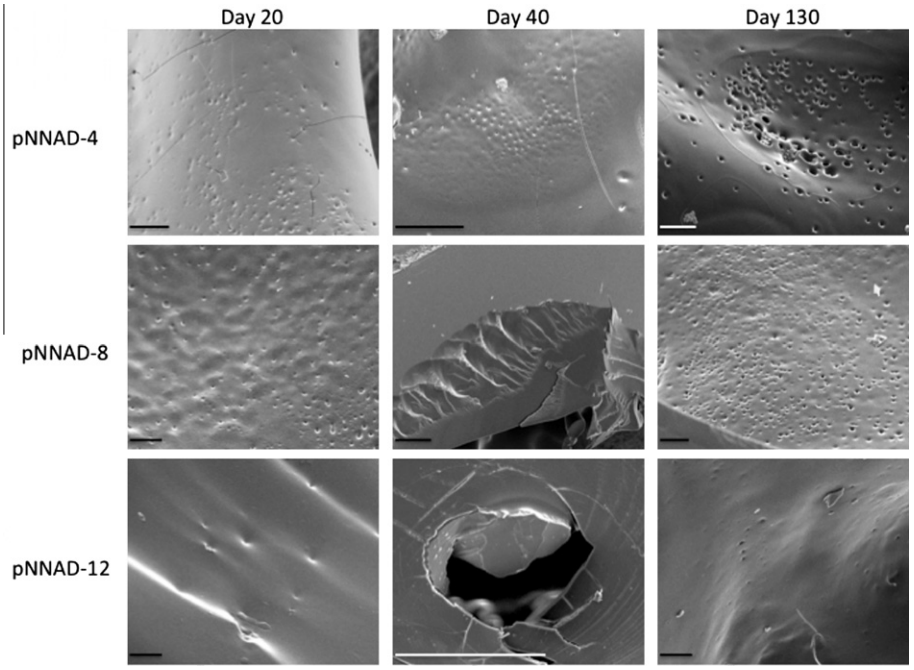

Fig. 7. SEM micrographs reveal subtle changes in copolymer surface morphology, indicative of the limited degradation that occurred over the 130 days in 37 °C PBS. Scale bar: 100 μm.

The copolymer drug loading efficiency was calculated by determining the dexamethasone concentration in the collected supernatant from the initial gel formation and from the PBS rinse prior to commencement of the assay. All three scaffolds demonstrated excellent loading capabilities, with pNNAD-4, pNNAD-8, and pNNAD-12 gels successfully entrapping 93.2%, 94.4%, and 96.0% of the initially infused dexamethasone. As expected, the pNNAD dexamethasone release curve reveals a small initial burst, which could potentially be helpful in treating the initial hostile environment within the compromised eye by decreasing the elevated VEGF expression and stabilization of the BRB, Fig. 8. However, as with all steroids, a large burst would not be desirable and therefore the burst must be controlled. The subsequent stabilization in the release curve that is observed around day 3 to 4, appears to produce the desired slow-releasing scaffold capable of maintaining low levels of drug that are sufficient to sustain a therapeutic concentration within the vitreous for extended periods of time. From day 5 to 24, the release rates were calculated to be 0.18, 0.09, and 0.16 μg day^{-1} for pNNAD-4, pNNAD-8, and pNNAD-12 respectively. These release rates are similar to studies performed by Alimera Sciences (Appharetta, GA, USA) examining the release of 0.2 μg day^{-1} fluocinolone acetonide (FA) from the non-degradable intravitreal insert, Iluvien [31]. They found that the low levels of corticosteroid were sufficient to produce a reduction in edema and improvements in visual acuity [31]. Furthermore, it was reported that a similar scaffold releasing slightly higher doses of FA (0.5 μg day^{-1}) were associated with mild increases in IOP, whereas the low level insert did not produce any elevation in pressure [31]. Therefore, it is likely that the low levels of corticosteroid released from the pNNAD scaffold following the initial burst are favorable for posterior segment delivery provided that the concentration within the vitreous is sufficient to produce a lasting therapeutic effect while minimizing complications associated with free drug exposure. We envision that the low levels released from the slow-degrading pNNAD copolymers will offer an improvement in release time over currently available degradable systems, and will approach, but likely not match, the sustained release of non-degrading Iluvien. However, such information will need to be elucidated through long-term drug release assays, future animal studies and optimization of polymer/drug conditions. Further in vitro investigation will examine the release of different therapeutics, such as anti-VEGF agents and other protein-based drugs that have demonstrated promise in the treatment of ocular diseases. Although less than 20% of the drug had been released after 24 days, this release study had to be terminated prematurely due to improper sample capping, leading to loss of liquid. However, the samples remained intact and long-term release studies are ongoing.

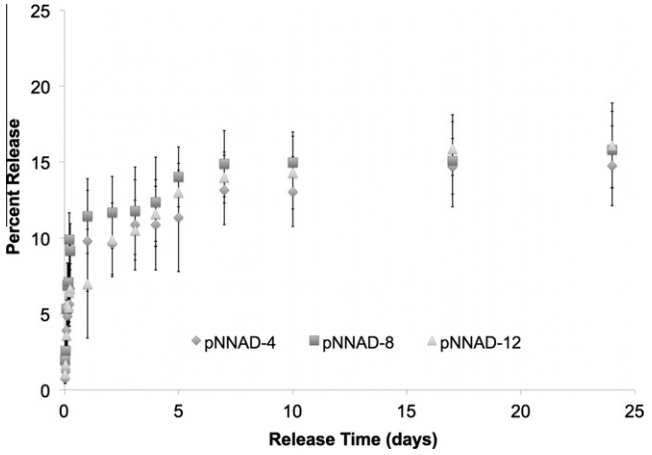

Fig. 8. Dexamethasone release from the various pNNAD scaffolds. An initial burst phase is observed followed by stabilization, which would ideally be capable of providing low levels of drug within the vitreous for sustained periods of time.

3.8. In vitro cell viability

In vitro testing of the pNNAD copolymers revealed excellent compatibility with RPE cells, as shown in Fig. 9. Copolymer scaffolds were dissolved in the supernatant of pre-adhered cells and

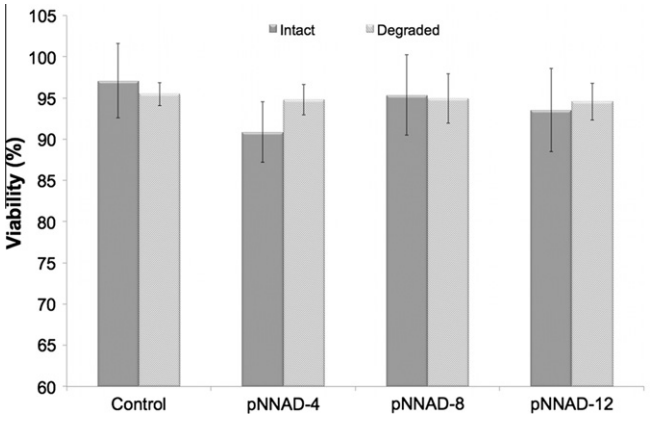

Fig. 9. Both intact and fully degraded pNNAD copolymers demonstrate excellent compatibility with RPE cells in culture. Partially degraded pNNAD was also found to be highly compatible with RPE cells (data not shown).

incubated for 96 h. Viability remained above 90% for all samples tested. Additionally, RPE cells were found to be compatible in culture with the copolymers as they transition through the various stages of hydrolytic degradation from partial to complete hydrolysis (partially degraded pNNAD data not shown). While these preliminary studies were designed to establish a safety profile for subsequent animal testing and demonstrate the compatibility of pNNAD scaffolds with RPE cells in culture, future studies will examine the potential use of cell-adhesive pNNAD formulations that possess the ability to act as temporary cell scaffolds. Subsequent studies have revealed that bioconjugation of pNNAD copolymers with cell adhesive RGDS peptides can easily be achieved through coupling the peptide with the amine-reactive NAS comonomer (data not shown). Future studies will examine the potential of RGDS-conjugated pNNAD scaffolds to support and maintain a healthy, functional population of RPE cells in vitro and within the subretinal space in vivo.

3.9. Subcutaneous implantation in mice

In accordance with the McMaster University Animal Research Ethics Board, prior to testing pNNAD copolymers in an ophthalmic application, demonstration of initial copolymer safety was required. Therefore, preliminary in vivo testing of pNNAD-4, pNNAD-8 and pNNAD-12 was performed via subcutaneous injection above the left flank of either C3H (day 1, 3 and 7) or SKH1-E (day 40) mice. All samples were successfully injected using a 25-gauge needle and formed a mechanically robust gel beneath the skin. The gel spread out into an apparent thin film underneath the skin quickly after injection, presumably as a result of being compressed between the dermis and underlying adipose tissue. For subretinal cell transplantation, scaffold spreading is favorable as it allows single injections to treat a relatively large area [32]. However, polymer spreading would not be suitable for drug delivery purposes, as a thin film with a large surface area would quickly release infused drug. In the absence of compressive forces, how-

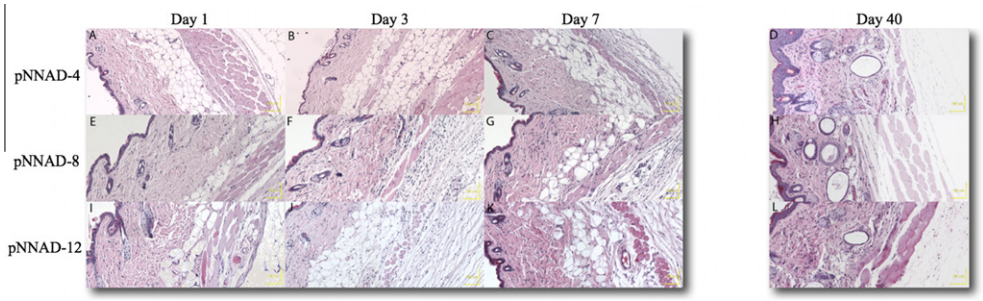

Fig. 10. Haemotoxylin and eosin staining of skin taken from the injection site of mice treated with pNNAD-4 (A–D), pNNAD-8 (E–H) and pNNAD-12 (I–L). From left to right, tissues were explanted 1, 3, 7 and 40 days post-implantation. Day 1, 3 and 7 samples were collected from the same litter of CH3 mice ($n = 3$), whereas day 40 samples were from hairless SKH1-E mice ($n = 2$). Scale bar = 100 μm.

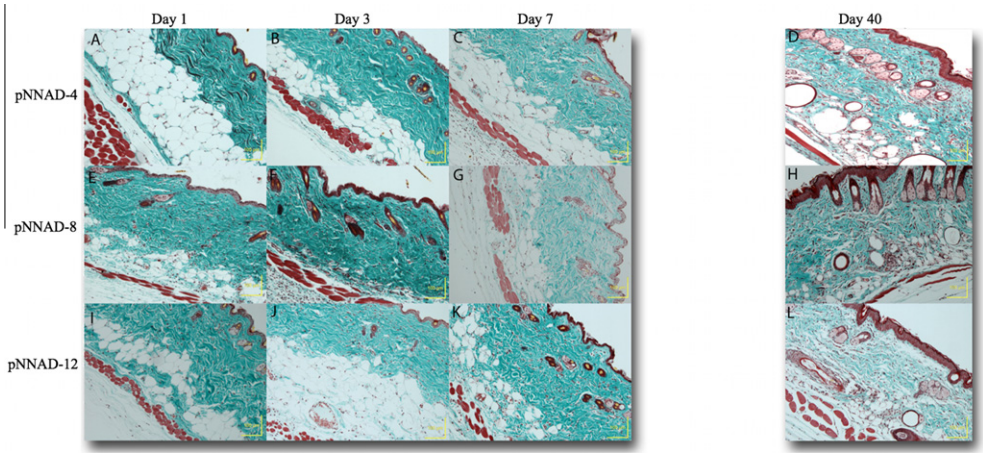

Fig. 11. Masson's trichrome staining of skin taken from the injection site of mice treated with pNNAD-4 (A–D), pNNAD-8 (E–H) and pNNAD-12 (I–L). From left to right, tissues were explanted 1, 3, 7 and 40 days post-implantation. Day 1, 3 and 7 samples were collected from the same litter of CH3 mice ($n = 3$), whereas day 40 samples were from hairless SKH1-E mice ($n = 2$). Scale bar = 100 μm.

Table 2
Mass of whole spleen and liver excised from SKH1-E mice after 40 days of subcutaneous incubation with pNNAD copolymers.

Sample	Liver		Spleen	
	Mass (g)	Body weight (%)	Mass (g)	Body weight (%)
Control	1.48	5.3	59	0.22
pNNAD-4	1.43	5.5	36	0.14
	1.33	5.1	61	0.23
pNNAD-8	1.55	5.3	51	0.17
	1.51	5.1	55	0.19
pNNAD-12	1.49	5.3	29	0.10
	1.41	5.1	39	0.15

ever, such as in the drug release and degradation assays, polymer thinning was not observed and the gels maintained their shape throughout the duration of the experiments. The absence of compressive forces within the intravitreal space would therefore be expected to allow injected copolymers to maintain their gelled morphology; this will be examined in future studies.

While material spreading is desirable for subretinal cell therapy, it made identification of the injected copolymer and subsequent histological analysis of the surrounding tissues difficult. Therefore tissue sections were obtained by excising and analyzing tissue from the injection site, which had previously been marked with indelible marker. Histological analysis of tissue at the injection site revealed evidence of a mild inflammatory response to subcutaneous injections characterized primarily by the presence of lymphocytes. Control samples, which received injections of equivalent volumes of saline, did not exhibit such inflammation. However, inflammation in the pNNAD-receiving mice appeared to subside by day 7 and was absent in the 40-day post-injection samples. Furthermore, there was very little macrophage accumulation or fibroblastic proliferation, indicating an acceptable, non-chronic immune response, which was consistent between all three pNNAD materials tested. DBA content did not exert an apparent effect on tissue response to pNNAD copolymers.

While day 1, 3, and 7 samples were collected from the same litter of C3H mice, the 40-day samples were from a nude SKH1-E mouse. The hairless SKH1-E mice were initially used to allow visualization of the skin during injection and to track copolymer location following implantation. However, in subsequent studies, C3H mice were simply shaved to remove hair from the injection site, allowing easy visualization of injection and copolymer tracking, thus eliminating the requirement for a hairless mouse. The distinction in mouse type is important when viewing the tissue sections as they yield substantially different dermal histology. SKH1-E mice have large, vacuolated spaces present from aborted hair follicles, which can be misconstrued as pockets of foreign material [33]. Therefore, SKH1-E and C3H histology images have been separated by a space in Figs. 10 and 11. There was no observable fibrous scar reaction, and trichrome staining confirms that collagen present appears to be type 1, characterized by regular, thick, wavy bundles. These results show a good in vivo tolerance to pNNAD copolymers, and suggest an absence of toxicity or chronic immune activation.

Although analysis of the injection site revealed acceptable histological results, the inability to directly locate non-staining pNNAD copolymers warranted an investigation of distal organs responsible for sequestering and clearing foreign materials. Whole spleen and liver were therefore excised from mice at day 40 and, after visual examination, were weighed. Neither spleen nor liver demonstrated signs of atrophy or inflammation and masses were consistent between the mice, Table 2. Future studies will employ fluorophore-conjugated pNNAD copolymers to allow accurate copolymer identification.

4. Conclusions

Several thermoresponsive copolymers based on NIPAAm, NAS and varying compositions of AA and DBA were synthesized for application in posterior segment ophthalmic cell and drug therapeutics. These copolymers were designed to address the serious need to improve upon current ophthalmic drug delivery approaches. All pNNAD copolymers possess sub-physiological phase transition temperatures, allowing minimally invasive delivery of drug-infused polymer suspensions into the back of the eye, followed by a temperature-induced scaffold formation, entrapping the pharmaceutical and creating a solid intravitreal drug depot. The slow degrading pNNAD copolymers were designed to provide a localized, sustained-release scaffold capable of maintaining therapeutically relevant doses of pharmaceutical within the vitreous, thereby minimizing the frequency of intervention and decreasing the associated risks. Degradation of the pNNAD copolymers was observed to occur through a simple hydrolytic opening of the DBA ring, resulting in an LCST increase that initiates scaffold rehydration and clearance from the body without the need for secondary surgical intervention or the production of low molecular weight degradation products. The copolymers did not appear to elicit an observable adverse response following subcutaneous injection into SKH1-E and C3H mice. Therefore, the preliminary safety profile and promising results warrant further investigation of these copolymers in an ocular environment. Future studies will examine in vitro drug release profiles using a number of different pharmaceuticals and protein-based therapeutics. In addition, we will look at histological analysis of ocular tissues and intravitreal distribution of drug following injection of pNNAD copolymers into the vitreous chamber.

Disclosures

Heather Sheardown is the founder of the 20/20 NSERC Ophthalmic Materials Network, which has ties with and receives funding from the following industrial partners: Alimera Sciences, CIBA Vision Corporation, Custom Contact Lenses, Fovea Pharmaceuticals, iCo Therapeutics, Siltech Corporation, Take Control Cosmedix, Vista Optics Limited and Walsh Medical Devices Incorporated.

Acknowledgements

The authors would like to acknowledge NSERC as well as the NSERC 20/20 Ophthalmic Materials Network for funding.

Appendix A. Figures with essential colour discrimination

Certain figures in this article, particularly Figs. 10 and 11, are difficult to interpret in black and white. The full colour images can be found in the on-line version, at http://dx.doi.org/10.1016/j.actbio.2012.03.018.

References

[1] Schwartz SG, Flynn Jr HW. Pharmacotherapies for diabetic retinopathy: present and future. ExpDiabetes Res 2007;2007:52487-1-8. http://dx.doi.org/10.1155/2007/52487.
[2] Del Amo EM, Urtti A. Current and future ophthalmic drug delivery systems. A shift to the posterior segment. Drug Discov Today 2008;13:135–43.
[3] Urtti A. Challenges and obstacles of ocular pharmacokinetics and drug delivery. Adv Drug Deliv Rev 2006;58:1131–5.
[4] Gaudana R, Jwala J, Boddu SH, Mitra AK. Recent perspectives in ocular drug delivery. Pharm Res 2009;26:1197–216.
[5] Choonara YE, Pillay V, Danckwerts MP, Carmichael TR, du Toit LC. A review of implantable intravitreal drug delivery technologies for the treatment of posterior segment eye diseases. JPharmSci 2009;99:2219–39.

[6] Morais JM, Papadimitrakopoulos F, Burgess DJ. Biomaterials/tissue interactions: possible solutions to overcome foreign body response. AAPS J 2010;12:188–96.
[7] Kang Derwent JJ, Mieler WF. Thermoresponsive hydrogels as a new ocular drug delivery platform to the posterior segment of the eye. Trans Am Ophthalmol Soc 2008;106:206–13.
[8] Jardeleza MS, Miller JW. Review of anti-VEGF therapy in proliferative diabetic retinopathy. Semin Ophthalmol 2009;24:87–92.
[9] Fitzpatrick SD, Mazumder MAJ, Lasowski F, Fitzpatrick LE, Sheardown H. PNIPAAm-grafted-collagen as an injectable, in situ gelling, bioactive cell delivery scaffold. Biomacromolecules 2010;11:2261–7.
[10] Neradovic D, Hinrichs WLJ, Kettenes-van den Bosch JJ, Hennink WE. Poly(N-isopropylacrylamide) with hydrolyzable lactic acid ester side groups: a new type of thermosensitive polymer. Macromol Rapid Commun 1999;20:577–81.
[11] Neradovic D, van Steenbergen MJ, Vansteelant L, Meijer YJ, van Nostrum CF, Hennink WE. Degradation mechanism and kinetics of thermosensitive polyacrylamides containing lactic acid side chains. Macromolecules 2003;36:7491–8.
[12] Ma Z, Nelson DM, Hong Y, Wagner WR. Thermally responsive injectable hydrogel incorporating methacrylate-polylactide for hydrolytic lability. Biomacromolecules 2010;11:1873–81.
[13] Yoshida T, Aoyagi T, Kokufuta E, Okano T. Newly designed hydrogel with both sensitive thermoresponse and biodegradability. J Polym Sci Part A-Polym Chem 2003;41:779–87.
[14] Cui ZW, Lee BH, Vernon BL. New hydrolysis-dependent thermosensitive polymer for an injectable degradable system. Biomacromolecules 2007;8:1280–6.
[15] Cui Z, Lee BH, Pauken C, Vernon BL. Manipulating degradation time in a N-isopropylacrylamide-based co-polymer with hydrolysis-dependent LCST. J Biomater Sci Polym Ed 2010;21:913–26.
[16] Mathy V. Biological evaluation of medical devices: identification and quantification of degradation products from polymeric medical devices. Geneva, Switzerland: 3rd ed. New york: International Organization for Standardization; 1998.
[17] Quiram PA, Gonzales CR, Schwartz SD. Severe steroid-induced glaucoma following intravitreal injection of triamcinolone acetonide. Am J Ophthalmol 2006;141:580–2.
[18] Thompson JT. Cataract formation and other complications of intravitreal triamcinolone for macular edema. Am J Ophthalmol 2006;141:629–37.
[19] Ruggiero A, Villa CH, Bander E, Rey DA, Bergkvist M, Batt CA, et al. Paradoxical glomerular filtration of carbon nanotubes. Proc Natl Acad Sci USA 2010;107:12369–74.
[20] Shah CA. Diabetic retinopathy: a comprehensive review. Indian J Med Sci 2008;62:500–19.
[21] Lee SS, Robinson MR. Novel drug delivery systems for retinal diseases. A review. Ophthalmic Res 2009;41:124–35.
[22] Kuppermann BD. Toxicity studies on triamcinolone acetonide and dexamethasone. Retina Today 2010:4–13.
[23] Sharma A, Pirouzmanesh A, Patil J, Estrago-Franco MF, Zacharias LC, Pirouzmanesh A, et al. Evaluation of the toxicity of triamcinolone acetonide and dexamethasone sodium phosphate on human lens epithelial cells (HLE B-3). J Ocul Pharmacol Ther 2011;27:265–71.
[24] Patil AJ, Mansoor A, Sharma A, Kuppermann BD. Effects of dexamethasone on human trabecular meshwork cells in vitro. Fort Lauderdale, FL: Association for Research in Vision and Ophthalmology annual meeting; 2009.
[25] Narayanan R, Mungcal JK, Kenney MC, Seigel GM, Kuppermann BD. Toxicity of triamcinolone acetonide on retinal neurosensory and pigment epithelial cells. Invest Ophthalmol Vis Sci 2006;47:722–8.
[26] Zacharias LC, Luthra S, Dong J, Kuppermann BD. Effect of dexamethasone on mitochondrial func- tion and cell viability in human retinal pigment epithelial and rat neurosensory retinal cells in vitro. Fort Lauderdale, FL: Association for Research in Vision and Ophthalmology Annual Meeting; 2007.
[27] Schwartz SG, Flynn HW, Scott IU. Pharmacotherapy for diabetic retinopathy. Expert Opin Pharmacother 2009;10:1123–31.
[28] Beer PM, Bakri SJ, Singh RJ, Liu W, Peters Iii GB, Miller M. Intraocular concentration and pharmacokinetics of triamcinolone acetonide after a single intravitreal injection. Ophthalmology 2003;110:681–6.
[29] Morse LS, Modjtahedi S, Smit-McBride Z. Use of intravitreal steroids in the clinic. Retina Today 2010:6–10.
[30] Haller JA, Kuppermann BD, Blumenkranz MS, Williams GA, Weinberg DV, Chou C. Randomized controlled trial of an intravitreous dexamethasone drug delivery system in patients with diabetic macular edema. Arch Ophthalmol 2010;128:289–96.
[31] Campochiaro PA, Hafiz G, Shah SM, Bloom S, Brown DM, Busquets M, et al. Sustained ocular delivery of fluocinolone acetonide by an intravitreal insert. Ophthalmology 2010;117:1393–9.
[32] Ballios BG, Cooke MJ, van der Kooy D, Shoichet MS. A hydrogel-based stem cell delivery system to treat retinal degenerative diseases. Biomaterials 2009;31:2555–64.
[33] Sorg H, Krueger C, Vollmar B. Intravital insights in skin wound healing using the mouse dorsal skin fold chamber. J Anat 2007;211:810–8.